Impact of S-CO₂ Properties on Centrifugal Compressor Impeller: Comparison of Two Loss Models for Mean Line Analyses

Akshay Khadse, Lauren Blanchette, Mahmood Mohagheghi, Jayanta Kapat
Center for Advanced Turbomachinery and Energy Research (CATER) Laboratory for Cycle Innovation and Optimization, University of Central Florida, Orlando, Florida 32816, USA

Akshay Khadse

Akshay Khadse is a Ph.D. candidate in Mechanical engineering at the University of Central Florida. He is currently working as a Graduate Research Assistant at the Center for Advanced turbomachinery and Energy Research, performing research on S-CO₂ power cycles as well as gas turbine trailing edge fin cooling. He completed his Bachelors and Masters of Technology from Indian Institute of Technology Bombay, India.

Lauren Blanchette

Lauren is a Master of Science degree candidate in Mechanical Engineering at the University of Central Florida (UCF). She is also a Graduate Research Assistant at the Center for Advanced turbomachinery and Energy Research, performing research on S-CO₂ power cycles as well as impingement heat transfer for intercooling applications. She received her Bachelor of Science in Mechanical Engineering at UCF as well.

Mahmood Mohagheghi

Mahmood received his first M.Sc. in Energy Systems Engineering from Sharif University of Technology and second M.Sc. in Mechanical Engineering from University of Central Florida. He currently works as a research assistant and Ph.D. candidate at University of Central Florida. Mahmood's primary research areas are S-CO2 power cycles, waste heat to power, combined heat and power, heat recovery steam generator, solar thermal energy, concentrated solar power, modeling and optimization of thermal power plants, thermo-economics, exergy analysis, and genetic algorithm.

Jayanta Kapat

Prof Jay Kapat is the Lockheed Martin Professor in the Department of Mechanical & Aerospace Engineering at the University Of Central Florida (UCF). He is the Founding Director for the Center for Advanced Turbomachinery and Energy Research (CATER). He is also the Associate Director of the Florida Center for Advanced Aero-Propulsion (FCAAP). His own research is focused on (a) heat transfer, aerodynamics and advanced cooling techniques for gas turbine engines, electrical generators and rocket engines, (b) supercritical carbon dioxide based power generation cycles and associated components, and (c) chemistry and performance characterization of alternative fuels for aviation. He joined UCF in 1997. Prior to that, Prof Kapat received Sc.D. from the Massachusetts Institute of Technology, MS from Arizona State University, and B.Tech. (Hons) from Indian Institute of Technology Kharagpur – all in Mechanical Engineering.

ABSTRACT

Accurate calculation of losses is one of the most critical part in the design process of any turbomachinery component. The amount of losses calculated not only decides the required outputs from the component, but also conveys the efficiency the component is projected to achieve. Considering modeling can become increasingly complex and expensive when an unconventional gas, such as supercritical carbon dioxide (S-CO_2), is of interest, a one dimensional analysis is utilized as the starting point of the design processes for any turbomachinery component. A one dimensional analysis can serve as a first estimate of the losses occurring within the component and ultimately the efficiency of the system. The present study provides a comparison between two mean line analysis methods for the design of a centrifugal compressor impeller with S-CO_2 as the working fluid. The main difference between the two analysis methods is the correlations used to calculate the losses occurring in the impeller. While method A calculates internal losses solely in terms of work loss, method B depends on relative total pressure losses for the calculation of internal losses and hence the comparison serves to find the impact the discrepancies between the two loss models chosen has on the results. The main centrifugal compressor in reference to a 100 MW S-CO_2 closed loop Recuperated Recompression Brayton cycle is investigated. Given the conditions at inlet of the main compressor stage, conditions at the impeller exit are derived through the two previously mentioned mean line analysis methods for target pressure ratio and rotation speed relative to the specified cycle. The results from the two loss models are compared and presented here. The significant difference is found in the resultant impeller pressure ratio, where method A gives a ratio of 2.49 while in method B, which updates the pressure ratio using the calculated pressure losses, a pressure ratio of 2 is observed. This work displays the need for more in-depth analysis, aided by detailed computational fluid dynamics (CFD) with real gas proper2ties and validated by detailed experimental data to further assess the ability of this performance model to capture all the losses.

INTRODUCTION

With the demand for electricity relentlessly increasing and the need to limit environmental pollution, it is becoming vital to develop more efficient and cleaner energy saving solutions. One such way that researchers are attempting to meet the world's energy needs is by exploring alternative working fluids in power generation cycles, such as supercritical carbon dioxide (S-CO_2), that show potential to enhance cycle efficiency while lowering the capital cost and output pollution. The ability of S-CO_2 Brayton cycles to operate in a range of temperatures makes this cycle applicable in multiple power generation environments as the power conversion option. Some potential applications include concentrated solar power systems (CSP), nuclear reactors, and waste heat recovery. Turchi et al.[1] has studied S-CO_2 Brayton cycles for application of CSP extensively and explains the advantages of S-CO_2 power cycles when compared to steam cycles. The study included more simple plant design compared to Rankine cycles along with higher efficiencies, and smaller size and volume due to the high density of carbon dioxide at the specified operating conditions. S-CO_2 power cycles present promising potential for next generation power cycles. S-CO_2 cycles require relatively low power for compression with inlet operating conditions close to the fluid's critical point, T=304.13 K and P=7.69 MPa[2]. For S-CO_2 Brayton cycles, 25-30% of the gross power produced from the turbine is usually spent to operate the compressor versus the usual 45% or so of other current working fluids such as helium, its competitor in nuclear reactor systems[2]. As a result, it has been observed that the amount of research being performed on the possible cycle configuration and optimization is expanding. Turchi et al. [1] and Mohagheghi and Kapat[3] studied different cycle configurations and optimization tools to assess the most practical power cycle designs for solar tower applications. Dostal et al.[4] presents a significant decrease in the turbine size and

system complexity for S-CO$_2$ power cycles when compared to helium and steam power cycles. Due to the higher efficiency when compared to the simple Recuperated cycle and simpler cycle layout than more complex S-CO$_2$ cycle designs, a closed loop Recuperated Recompression (RRC) Brayton cycle with a net output of 100 MW and an inlet turbine temperature (TIT) of 1350 K was chosen to carry out this study. Through the methodology developed by Mohagheghi et al.[5], the cycle states are obtained for the cycle under investigation. Table 1 displays the results of this cycle calculation and Fig. 1 displays the cycle configurations along with the resulting T-s diagram, connecting lines for this diagram are not exact, just schematic.
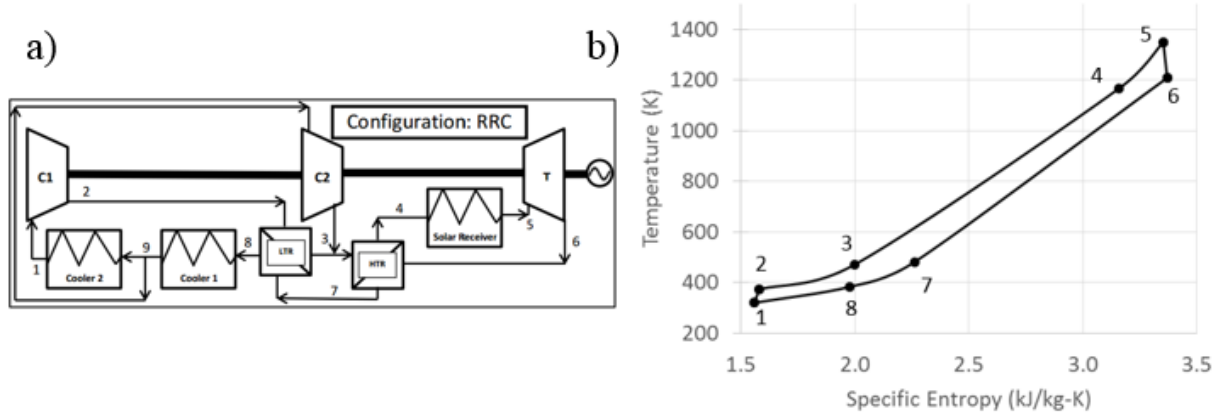

**Figure 1. a) Recuperated Cycle Layout[5] and b) Corresponding T-s Diagram**

Table 1. Tabulated Cycle States for the Specified Recuperated Recompression Cycle

State Points	Temperature (K)	Pressure (kPa)	Specific Enthalpy (kJ/kg)	Density (kg/m^3)	Specific Entropy (kJ/kg-K)
1	320.0	9500	382.5	374.26	1.58
2	378.9	24000	420.5	544.16	1.60
3	487.9	23976	606.8	295.75	2.03
4	1154.4	23952	1455.6	103.75	3.13
5	1350.0	23904	1713	88.59	3.34
6	1196.6	9691	1511.8	41.91	3.36
7	498.2	9643	662.9	109.33	2.31
8	388.9	9595	529.7	162.65	2.00

Further studies have been performed on the individual components within the cycle to determine the impact S-CO$_2$ has on the performance and effects on operation of these parts. Schmitt et al.[6] aimed to design a first stage turbine vane for the use in an S-CO$_2$ Recuperated Cycle while Carlson et al.[7] explains the experiment being performed at Sandia National Laboratories on Heat Exchanges for this cycle. Experiments of S-CO$_2$ centrifugal compressors can become costly due to the high operating pressures of S-CO$_2$. The development of a 1-D analysis, tailored specifically to S-CO$_2$ power cycles to assess the aerodynamic performance of the compression system accurately would aid in further

advancement with this unexploited field. Due to the complexity of the simulation, only a few numerical studies have been performed with the objective of modeling S-CO_2 centrifugal compressors. As displayed in Figure 2, the fluctuations of S-CO_2 thermodynamic properties, such as specific heat and viscosity, within the desired operating conditions for S-CO_2 Brayton cycles makes modeling the compressible real gas essential for accurate results. Brenes[8] devoted his research to designing an S-CO_2 centrifugal compressor in which he studies 1-D and 3-D numerical models that can be used for the design process. Through his work, he developed a step by step procedure to obtain numerical stability when performing a 3-D computational fluid dynamics (CFD) study of an S-CO_2 compressor impeller blade at operating conditions slightly above the fluid's critical point as well as a mean line analysis methodology. He validates his methodologies against the few experimental results publically available from the S-CO_2 compressor loop at the Sandia National Laboratory[9].

While Brenes[8] utilized work loss and pressure loss based loss calculation method, Sanghera[10] developed a mean line analysis method utilizing a loss calculation method solely dependent on work losses. The results from Sanghera's study were validated against the Eckardt O-Rotor, a centrifugal impeller experiment[10]. Although the results displayed acceptable agreeance with air, the Eckardt O-Rotor experiment was not carried out with S-CO_2 as the working fluid and thus a comparison could not be performed with this unconventional gas.
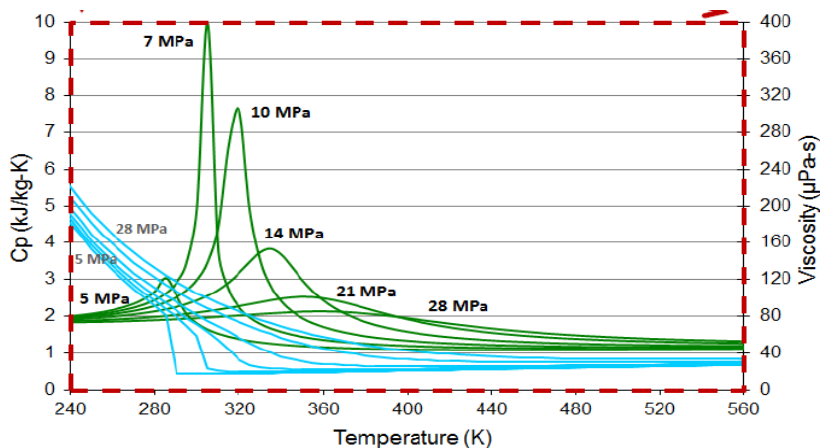
Figure 2. Viscosity & Specific heat Property variation of CO_2 [6]

This study aims to make a comparison of two mean line analyses, method A with impeller parasitic and internal losses accounted for though work loss correlations and method B utilizing relative total pressure loss correlations to account for internal losses and work loss correlations to account for parasitic losses. Through this study, the agreeance between the two types of analysis will be determined. Further Explanation in the differences between the two analyses are shown through comparable h-s diagram schematic in Figure 3 and Figure 4.
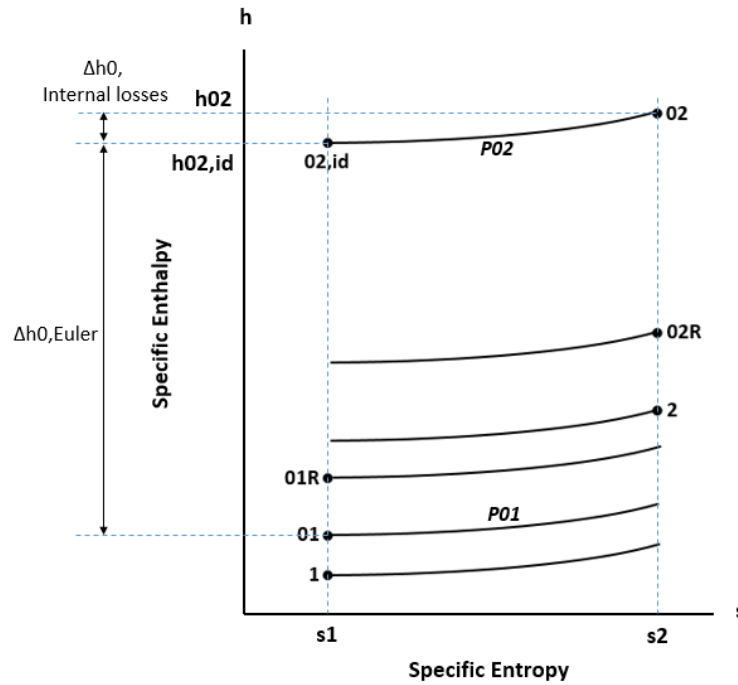
Figure 3. h-s Diagram Schematic for Method A; State 1 and 2 are Impeller Inlet & Exit Respectively
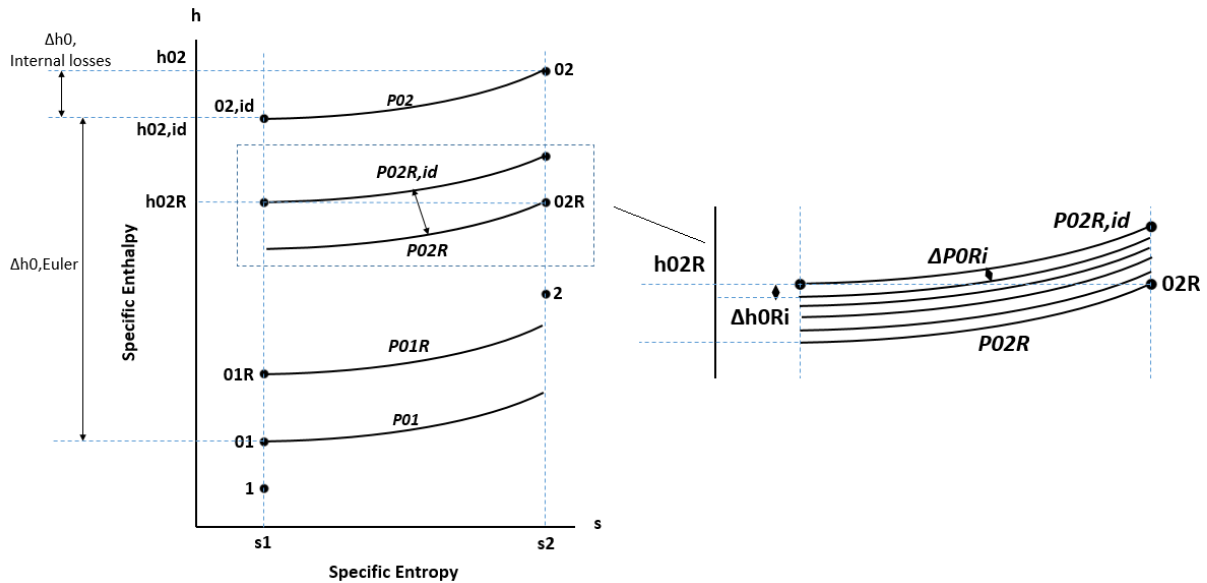
Figure 4. h-s Diagram Schematic for Method B; State 1 and 2 are Impeller Inlet & Exit Respectively

ANALYSIS METHODOLOGY

Calculation of losses in the centrifugal compressor is an important task to get a correct estimation of efficiency and pressure output. Internal losses as well as parasitic losses occur in a centrifugal compressor, causing entropy generation and total pressure losses. These are considered in the analysis for the presented work. Internal losses originate due to non-ideal behavior of the flow; while parasitic losses arise from mechanical deficiencies in impeller, reducing total enthalpy rise of the fluid as

compared to mechanical work input by the shaft. Hence parasitic losses do not exist for stationary components of a compressor. Internal losses include incidence losses, aerodynamic loading losses, skin friction losses, tip leakage losses and mixing losses. Parasitic losses comprises of disk friction losses, recirculation losses and seal leakage losses. For the sake of completeness and ease of comparison between the two methods, relevant details of the method as applicable for the impeller of this paper are presented below.

The mean line analysis codes are developed in MATLAB[11] based on law of conservation of mass, Euler Turbine equation, and centrifugal compressor loss models given in literature. The MATLAB[11] codes utilizes NIST REFPROP[12] database to solve equation of state at specified points for S-CO_2. Table 2 presents the input and output variables in the developed MATLAB[11] code. Various geometrical parameters used in the mean line analyses are shown in Fig. 5.

Table 2. Input and Output Variables for the Mean Line Analysis Code

Inputs	Outputs
▪ *Input Parameter* 　● T_{01}, P_{01} 　● Mass flow rate 　● Geometry parameters ▪ *Input Variables* 　● RPM	▪ Impeller exit conditions ▪ Converged Efficiency ▪ Compressor Impeller Pressure ratio
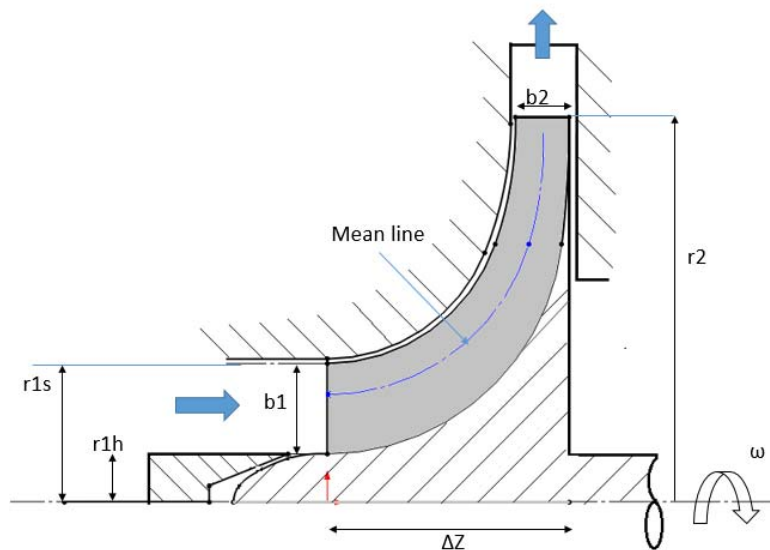
Figure 5. Schematic of the Centrifugal Compressor Impeller

Using the isentropic exit conditions, for a given value of RPM the impeller exit total pressure can be estimated. To set a value of RPM a total pressure ratio of 2.5 is chosen which is very close to the required compression ratio for the mentioned RRC Brayton cycle.

Table 3. Input and Output Variable Tabulated Values for Mean Line Analysis Code

Main Input Parameters and Variables	
T_{01}	320 K
P_{01}	9.5 MPa
Mass flow rate	472.189 kg/s
Angular Speed	6560 RPM
Main Geometrical Parameters	
r_{1h}	0.1322 m
r_{1s}	0.1924 m
r_2	0.2635 m
ΔZ	0.144 m
Z	15
b_2	0.0231 m
t	5.7 mm

A. Mean Line Analysis Based on Work Loss Model Methodology

All impeller losses for this loss calculation method are calculated in terms of work losses. The selected correlations for loss models have been proven to be accurate enough for use in the design of S-CO_2 compressors by Sanghera[10].

Incidence losses occur when the direction of relative velocity of fluid does not match with the inlet blade angle and therefore fluid cannot enter the blade passage smoothly by gliding along the blade surface. The direction of the relative velocity of the fluid is assumed to be congruent with the leading edge blade angle and thus incidence losses are not present in either mean line design analysis methods.

Aerodynamic loading losses can be described as momentum loss due to boundary layer buildup (Jansen[13]) and arise from deflection of streamlines inside the impeller. These losses are evaluated using the model proposed by Coppage et al.[14], the correlation is presented in Eqn. 1.1.

$$\Delta h_{ABL} = 0.05 D_f^2 U_2^2 \qquad \text{[Equation 1.1]}$$

Where the Diffusion factor, D_f is defined as:

$$D_f = 1 - \frac{V_2}{V_{1,s}} + \frac{0.75\Delta h/U_2{}^2}{\left(\frac{V_{1,s}}{V_2}\right)\left[\frac{Z}{\pi}\left(1-\frac{r_{1,s}}{r_2}\right)+2\frac{r_{1,s}}{r_2}\right]} \qquad \text{[Equation 1.2]}$$

Skin friction losses are calculated using a relation given by Jansen[13], and defined in Eqn. 1.3.

$$\Delta h_{SF} = 2C_f \frac{L_b}{D_h} \bar{V}^2 \qquad \text{[Equation 1.3]}$$

Where the coefficient of fiction, C_f is given by Schlichting[15] [Eqn. 1.4] and Reynolds number is dependent on the hydraulic diameter, D_h. Calculation of the length of the blade along the mean line, L_b, is describe in Eqn. 1.5.

$$\frac{1}{\sqrt{4C_f}} = -2log_{10}\left[\frac{2.51}{Re_{D_h}\sqrt{C_f}}\right] \qquad \text{[Equation 1.4]}$$

$$L_b = \Delta Z - \frac{b_2}{2} + \frac{(r_1 - r_2)}{\cos(\beta_2)} \qquad \text{[Equation 1.5]}$$

Leakage of fluid from the pressure side to the suction side of the blade through the small gap between the tip of the blade and the casing is inevitable for open impellers which is the cause for tip clearance losses. The correlation given by Jansen[13] is used in this method:

$$\Delta h_{TCL} = 0.6 \frac{\delta_{TCL}}{b_2} \sqrt{\frac{4\pi}{b_2 Z} \left[\frac{r_{1,s}^2 - r_{1,h}^2}{(r_2 - r_{1,s})\left(1 + \frac{\rho_2}{\rho_1}\right)}\right] C_{w,2} C_{z,1}} \qquad \text{[Equation 1.6]}$$

Mixing loss arises when the distorted flow mixes with the free stream flow. Johnston and Dean[16] based their loss model on abrupt expansion losses which utilizes wake fraction given by Lieblein et al.[17].

$$\Delta h_{MIX} = \frac{1}{1 + \lambda_s^2} \left(\frac{1 - \varepsilon_{wake} - \frac{b_3}{b_2}}{1 - \varepsilon_{wake}}\right) \frac{C_2^2}{2} \qquad \text{[Equation 1.7]}$$

Terms ε_{wake} and λ_s represent the wake friction of the blade-to-blade spacing and the swirl parameter respectively. Both are defined below:

$$\lambda = \frac{C_{w,2}}{C_{m,2}} \qquad \text{[Equation 1.8]}$$

$$\varepsilon_{wake} = 1 - \frac{C_{m,wake}}{C_{m,mix}} \qquad \text{[Equation 1.9]}$$

Where the definition of $C_{m,wake}$ and $C_{m,mix}$ can be found in Leiblein et al.[17].

The total change in enthalpy due to internal losses is calculated through the summation of all the individual losses.

$$\Delta h_{internal} = \Delta h_{ABL} + \Delta h_{SF} + \Delta h_{TCL} + \Delta h_{MIX} \qquad \text{[Equation 1.10]}$$

The rotating disk of impeller experiences frictional forces because of the fluid surrounding the disk which introduces parasitic losses to the compressor. Daily and Nece[18] have conducted experiments on a smooth plane disk enclosed within a right-cylindrical chamber to compute disk friction losses.

Their loss models are used to compute losses for the current study with f_{DF} representing the friction factor and Reynolds number being dependent on conditions at the impeller exit.

$$\Delta h_{DF} = f_{DF} \bar{\rho} \left(\frac{r_2^2 U_2^3}{4\dot{m}}\right) \qquad \text{[Equation 1.11]}$$

$$f_{DF} = \frac{0.0622}{Re_{DF}^{0.2}} \qquad \text{[Equation 1.12]}$$

Recirculation losses arise due to back flow at the impeller tip which is known to cause an increase in impeller work input. The recirculation loss coefficient given by Oh et al.[19] is used here [Eqn. 1.13].

$$\Delta h_{RC} = 0.02 D_f^2 U_2^2 \sqrt{\cot(\alpha_2)} \qquad \text{[Equation 1.13]}$$

Where the diffusion factor was defined in Eqn. 1.4.

Leakage loss due to the seal are defined here using correlation presented in Aungier[21].

$$\Delta h_{LL} = \frac{\dot{m}_{CL} V_{CL}}{2\dot{m}} U_2 \qquad \text{[Equation 1.14]}$$

The total enthalpy change due to parasitic losses is determined through the summation of all the individual losses [Eqn. 1.15].

$$\Delta h_{parasitic} = \Delta h_{DF} + \Delta h_{RC} + \Delta h_{LL} \qquad \text{[Equation 1.15]}$$

For the current study two types of efficiencies are considered for the comparison of effects of parasitic losses and internal losses. The first one accounts for the parasitic losses as the extra amount of work needed to drive the compressor and called here as design efficiency [Eqn. 1.17] while the second one considers actual work imparted to the flow called here as aerodynamic efficiency [Eqn. 1.18].

$$\Delta h_{Euler} = C_{w2} U_2 - C_{w1} U_1 \qquad \text{[Equation 1.16]}$$

$$\eta_{Design} = \frac{\Delta h_{Euler} - \Delta h_{internal}}{\Delta h_{Euler} + \Delta h_{parasitic}} \qquad \text{[Equation 1.17]}$$

$$\eta_{Aerodynamic} = \frac{\Delta h_{Euler} - \Delta h_{internal}}{\Delta h_{Euler}} \qquad \text{[Equation 1.18]}$$

Furthermore, the slip factor, σ is calculated based on work by Wiesner[20] with correction implemented by Aungier[21]. Equation 1.19 through 1.22 define parameters used here.

$$\sigma = 1 - \frac{\sin(\alpha_2)\sqrt{\sin(\beta_2)}}{Z^{0.7}} \qquad \text{[Equation 1.19]}$$

$$\sigma_{corr} = \sigma\left(\frac{\epsilon - \epsilon_{lim}}{1 - \epsilon_{lim}}\right) \qquad \text{[Equation 1.20]}$$

$$\epsilon_{lim} = \frac{\sigma - \sigma^*}{1 - \sigma^*} \qquad \text{[Equation 1.21]}$$

$$\sigma^* = \sin(37° + \beta_2) \qquad \text{[Equation 1.22]}$$

Figure 6 presents the algorithm for the mean line analysis based on the discussed loss models and the input parameters and variables.
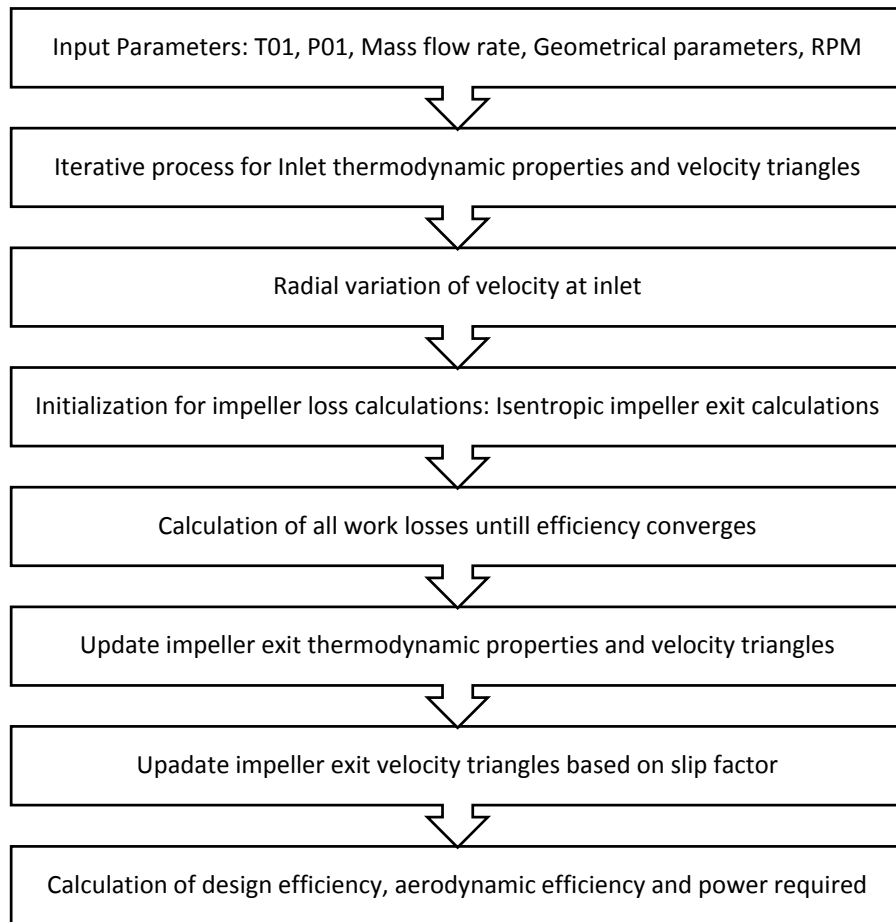
Figure 6. Algorithm for Mean-Line Analysis Code – Method A

B. Mean Line Analysis Based on Enthalpy and Pressure Loss Model Methodology

The second mean line analysis uses relative total pressure loss calculations to account for internal losses and work losses correlations to calculate parasitic losses. The selected correlations for this analysis method was validated for use in the design of S-CO$_2$ compressors by Brenes[8]. The losses are

calculated as non-dimensional terms, represented as ω and utilized in Eqn. 1.23 to calculate the relative total pressure at the outlet of the impeller.

$$P'_{02} = P'_{02,id} - f_c(P'_{01} - P_1)\sum_i \omega_i \qquad \text{[Equation 1.23]}$$

Through the calculation of relative total exit pressure, the absolute total pressure is obtained. This updates the ideal total enthalpy at the exit.

Skin friction losses and tip clearance losses are accounted for using correlations presented in Aungier[21] and are displayed in Eqn. 1.24 and Eqn. 1.25 respectively.

$$\omega_{SF} = 4C_f \frac{L_b}{D_h}(\frac{\bar{V}}{V_2})^2 \qquad \text{[Equation 1.24]}$$

$$\omega_{TCL} = \frac{2\dot{m}_{CL}\Delta p_{CL}}{\dot{m}\rho_2 V_2^2} \qquad \text{[Equation 1.25]}$$

Aerodynamic loading losses are accounted for by two terms, ω_{BL}, which accounts for the pressure gradient in the blade-to-blade direction, and ω_{HS}, which accounts for the pressure gradient from hub to shroud.

$$\omega_{BL} = \frac{1}{24}(\frac{\Delta V}{V_2})^2 \qquad \text{[Equation 1.26]}$$

$$\Delta V = \frac{2\pi D_2 U_2 I_b}{Z L_b} \qquad \text{[Equation 1.27]}$$

$$\omega_{HS} = (\frac{(\bar{\kappa}_m \bar{b}\bar{V})^2}{6V_2}) \qquad \text{[Equation 1.28]}$$

$$\omega_{ABL} = \omega_{BL} + \omega_{HS} \qquad \text{[Equation 1.29]}$$

Where ΔV is defined as the maximum relative velocity difference and is dependent on the blade work input coefficient, I_B, which is further explained in Equation 1.37 and $\bar{\kappa}_m$ is explained in Aungier[21].

Mixing losses are calculated for distorted flow inside the impeller as well as for the mixing of wake downstream of the trailing edge. The distorted flow losses are accounted for using correlation developed by Benedict et al.[22] [Eqn. 1.30] and the mixing of the wake downstream is calculated using correlation developed by Aungier[21] [Eqn. 1.31].

$$\omega_\lambda = [\frac{(\lambda-1)C_{m,3}}{V_2}]^2 \qquad \text{[Equation 1.30]}$$

$$\omega_{wake} = [\frac{C_{m,3,wake} - C_{m,3,mix}}{V_2}]^2 \qquad \text{[Equation 1.31]}$$

$$\omega_{MIX} = \omega_{wake} + \omega_\lambda \qquad \text{[Equation 1.32]}$$

The impeller exit relative total pressure is calculated through the sum of all the pressure loss coefficients and Equation 1.23.

Through work input coefficients, I derived from parasitic work losses, including disk friction losses, recirculation losses, leakage losses, and blade work input, the change in relative total enthalpy due to parasitic losses from impeller inlet to exit is calculated using Eqn. 1.33.

$$\Delta h_{0,parasitic} = U_2^2 \sum_{1\to2} I_i \qquad \text{[Equation 1.33]}$$

Disk friction losses are calculated using the relation modified by Aungier[21], originally presented by Daily and Nece[18].

$$I_{DF} = C_{MD}\frac{\rho_2 U_2 r_2^2}{2\dot{m}} \qquad \text{[Equation 1.34]}$$

Recirculation flow losses are estimated using correlation presented by Lieblein et al.[17].

$$I_{RC} = (\frac{D_{eq}}{2} - 1)(\frac{V_{w,2}}{C_{m,2}}) \qquad \text{[Equation 1.35]}$$

The correlation developed by Aungier[23] for leakage losses was used in this method.

$$I_{LL} = \frac{\dot{m}_{cL} C_{CL}}{2 U_2 \dot{m}}$$ [Equation 1.36]

The blade work input coefficient, the non-dimensional change of enthalpy of the fluid over the impeller, is calculated using correlation also given in Aungier[21] which utilizes slip factor and distortion factor. The overall total enthalpy change includes changes in enthalpy due to parasitic losses and blade work input.

$$I_B = \sigma \left(1 - \frac{\dot{m} \, \lambda \tan(\beta_2)}{\rho_2 A_2 U_2} \right) - \frac{U_1 C_{w,1}}{U_2^2}$$ [Equation 1.37]

Where the slip factor is calculated using Wiesner's Equation[20]

$$\Delta h_{0,Euler} = I_B * U_2^2$$ [Equation 1.38]

Further, the design and aerodynamic efficiencies are defined as:

$$\eta_{Design} = \frac{h_{02,id} - h_{01}}{\Delta h_{Euler} + \Delta h_{parasitic}}$$ [Equation 1.39]

$$\eta_{Aerodynamic} = \frac{h_{02,id} - h_{01}}{\Delta h_{Euler}}$$ [Equation 1.40]

The relative total enthalpy at impeller exit is calculated using the equation for conservation of rothalpy [Eqn. 1.38]. The entropy at the exit of the impeller can then be determined by the relative total pressure determined using Eqn. 1.23 and relative total enthalpy through the use of REFPROP[12] database for S-CO_2.

$$h_{02,R} = h_{01,R} + \frac{(U_2^2 - U_1^2)}{2}$$ [Equation 1.41]

Employing the equations discussed in this section within the Algorithm presented in Figure 7, the impeller exit conditions along with each losses contribution is determined. Further, the efficiency is computed. The slip factor is found utilizing the same correlations discussed in method A, through

Equations 1.19 to 1.22.

```
┌─────────────────────────────────────────────────────────────────────┐
│   Input Parameters: T01, P01, Mass flow rate, Geometrical parameters, RPM   │
└─────────────────────────────────────────────────────────────────────┘
                                  ↓
┌─────────────────────────────────────────────────────────────────────┐
│   Iterative process for Inlet thermodynamic properties and velocity triangles   │
└─────────────────────────────────────────────────────────────────────┘
                                  ↓
┌─────────────────────────────────────────────────────────────────────┐
│                  Radial variation of velocity at inlet                  │
└─────────────────────────────────────────────────────────────────────┘
                                  ↓
┌─────────────────────────────────────────────────────────────────────┐
│   Initialization for impeller loss calculations: Isentropic impeller exit calculations   │
└─────────────────────────────────────────────────────────────────────┘
                                  ↓
┌─────────────────────────────────────────────────────────────────────┐
│   Calculation of relative total pressure losses, work losses and blade work input   │
│                  coefficient untill efficiency converges                  │
└─────────────────────────────────────────────────────────────────────┘
                                  ↓
┌─────────────────────────────────────────────────────────────────────┐
│   Update impeller exit thermodynamic properties and velocity triangles   │
└─────────────────────────────────────────────────────────────────────┘
                                  ↓
┌─────────────────────────────────────────────────────────────────────┐
│        Upadate impeller exit velocity triangles based on slip factor        │
└─────────────────────────────────────────────────────────────────────┘
                                  ↓
┌─────────────────────────────────────────────────────────────────────┐
│   Calculation of  work losses due to internal losses by using relative total   │
│                          pressure losses                          │
└─────────────────────────────────────────────────────────────────────┘
                                  ↓
┌─────────────────────────────────────────────────────────────────────┐
│   Calculation of design efficiency, aerodynamic efficiency and power required   │
└─────────────────────────────────────────────────────────────────────┘
```

Figure 7. Algorithm for Mean-Line Analysis Code – Method B

RESULTS AND DISCUSSION

A. Results for Mean Line Analysis Based on Method A

Mean line analysis yields thermodynamic properties at impeller inlet and exit state points in the compressor stage which are presented in Table 4. A high value for compression ratio of 2.47 is observed for the impeller through this mean line analysis method.

Table 4. Thermodynamic Properties at Mentioned State Points for Method A

	Impeller Inlet conditions	Impeller Exit conditions
Total Pressure, P_0	9.5 MPa	23.42 MPa
Static Pressure P	9.5 MPa	17.44 MPa
Total Temperature, T_0	320 K	374.85 K
Static Temperature, T	319.49 K	357.15 K
Static Density, ρ	372.49 kg/m^3	297.91 kg/m^3
Static Enthalpy, h	382.28 kJ/kg	402.43 kJ/kg

Table 5 lists all the individual losses calculated for each loss type in the compressor impeller. These are calculated using loss correlations that are discussed in section A of the Methodology. Aerodynamic loading losses is determined to have the highest contribution to losses, while skin friction losses was found to be the least.

Table 5. Internal and Parasitic Work Losses Calculated Using Mean Line Analysis - Method A

Internal Work Losses	
Aerodynamic loading losses	1.05 kJ/kg
Skin friction losses	0.06 kJ/kg
Tip clearance losses	0.82 kJ/kg
Mixing losses	0.08 kJ/kg
Parasitic Work Losses	
Disk friction losses	0.09 kJ/kg
Leakage Losses	0.94 kJ/kg
Recirculation losses	0.10 kJ/kg

Through the summation of all the losses obtained, the impeller performance parameters were computed and listed in Table 6. The overall design efficiency was observed to be lower than the aerodynamic efficiency due to the parasitic losses accounted for within the design calculation.

Table 6. Efficiency and Power Calculation Using Mean Line Analysis –Method A

Slip Factor	0.87
Inlet Total Enthalpy, h_{01}	382.49 kJ/kg
$\Delta h_{0,Euler}$	31.36 kJ/kg
$\Delta h_{0,Internal}$	2.00 kJ/kg
Exit Ideal Total Enthalpy,$h_{02,id}$	411.84 kJ/kg
$\Delta h_{0,Parasitic}$	1.13 kJ/kg
Total-to-Total Efficiency (Design)	88.97%
Total-to-Total Efficiency (Aerodynamic)	93.60%
Power required	15.34 MW

B.   Mean Line Analysis Based on Enthalpy and Pressure Loss Model Results

Through mean line analysis method B, the resulting losses were calculated and the impeller exit conditions along with the impeller efficiency was ultimately determined. The impeller exit conditions determined are displayed in Table 7 while the performance parameters are displayed in Table 9. When relative total pressure loss correlations were used to define internal losses, a pressure ratio of 2 for the impeller was found.

Table 7. Thermodynamic Properties at Impeller Inlet and Exit State Points for Method B

	Impeller Inlet conditions	Impeller Exit conditions
Total Pressure, P_0	9.5 MPa	19.08 MPa
Static Pressure P	9.5 MPa	12.97 MPa
Total Temperature, T_0	320 K	360.22 K
Static Temperature, T	319.49 K	359.90 K
Static Density, ρ	372.49 kg/m^3	250.95 kg/m^3
Static Enthalpy, h	382.28 kJ/kg	393.56 kJ/kg

Individual internal loss coefficients along with parasitic work losses were calculated using the correlations presented in Section B of the Methodology. The results are displayed in Table 8. Similar to method A, it is observed that Aerodynamic losses have the highest contribution to internal losses while mixing losses have very little effect on the overall pressure loss.

Table 8. Internal and Parasitic Work Losses Calculated Using Mean Line Analysis - Method B

Internal Losses Coefficients, ω_i	
Aerodynamic loading losses	0.312
Skin friction losses	0.011
Tip clearance losses	0.047
Mixing losses	0.007
Parasitic Work Losses	
Disk friction losses	1.98 kJ/kg
Leakage Losses	0.83 kJ/kg
Recirculation losses	0 kJ/kg

Table 9. Efficiency and Power Calculation Using Mean Line Analysis – Method B

Slip Factor	0.87
Inlet Total Enthalpy, h_{01}	382.49 kJ/kg
$\Delta h_{0,Euler}$	24.00 kJ/kg
$\Delta h_{0,Internal}$	2.66 kJ/kg
Exit Ideal Total Enthalpy, $h_{02,id}$	403.83 kJ/kg
$\Delta h_{0,Parasitic}$	2.81 kJ/kg
Total-to-Total Efficiency (Design)	79.60%
Total-to-Total Efficiency (Aerodynamic)	12.66 MW
Power required	88.92%

C. Comparison of the two Mean Line Analysis Methodology

For comparison purposes, the individual relative pressure losses due to each internal loss for Method B were used to calculate the change in relative total enthalpy.

With the velocity triangles resulting from the converged inlet and exit impeller conditions, the change in relative total enthalpy was calculated to be equivalent to the change in absolute total enthalpy.

$$\Delta h_{02R,id\rightarrow02R} = \Delta h_{0R,SF} + \Delta h_{0R,TCL} + \Delta h_{0R,ADL} + \Delta h_{0R,MIX} \approx \Delta h_{02,id\rightarrow02} \qquad \text{[Equation1.38]}$$

In method B, the blade work input coefficient was used to calculate the total enthalpy change from impeller inlet to exit. This calculated value was compared to sum of the relative total enthalpy change due to internal losses within the method and less than 3% difference was observed.

Table 10. Internal and Parasitic Work Losses Calculated Using Mean Line Analysis Method B

Impeller Efficiency	Method A	Method B
Total-to-Total Efficiency (design)	87.66%	79.60%
Total-to-Total Efficiency (aerodynamic)	92.55%	88.92%
Internal Work Losses		
Aerodynamic loading losses	1.05 kJ/kg	2.19 kJ/kg
Skin friction losses	0.06 kJ/kg	0.073 kJ/kg
Tip clearance losses	0.82 kJ/kg	0.33 kJ/kg
Mixing losses	0.08 kJ/kg	0.072 kJ/kg
Parasitic Losses		
Disk friction losses	0.09 kJ/kg	1.98 kJ/kg
Leakage Losses	0.94 kJ/kg	0.83 kJ/kg
Recirculation losses	0.10 kJ/kg	0 kJ/kg
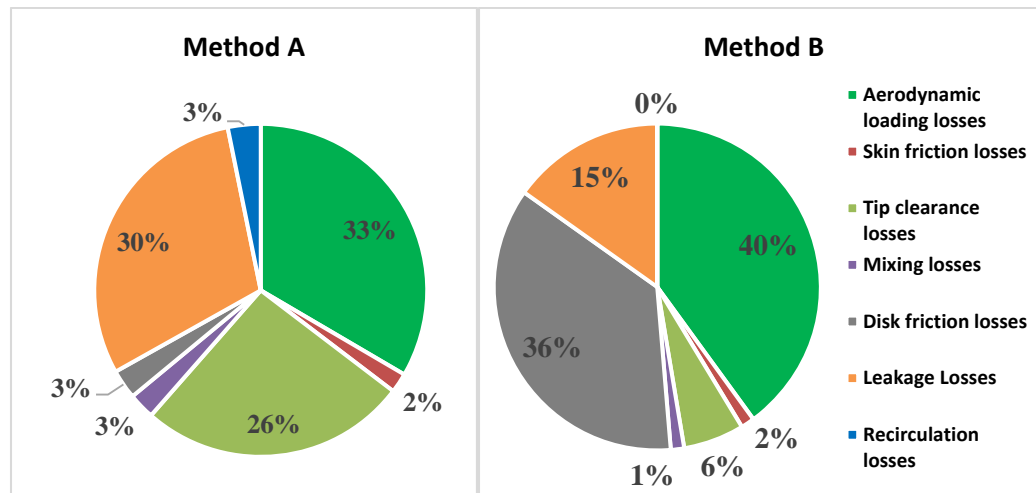
Figure 8. Comparison of Percentage for Each Resulting Loss from Method A and Method B

A significant difference between method A and method B is the resulting weight the disk friction losses plays in the overall losses determined, displayed in Figure 8. Results from Method A show small amount of losses due to disk friction, while disk friction plays an important role in method B. Due to the fact that design efficiency takes into account parasitic losses, the efficiency in method A comes out be to noticeably higher than seen in method B. This comparison can be observed in Table 10.
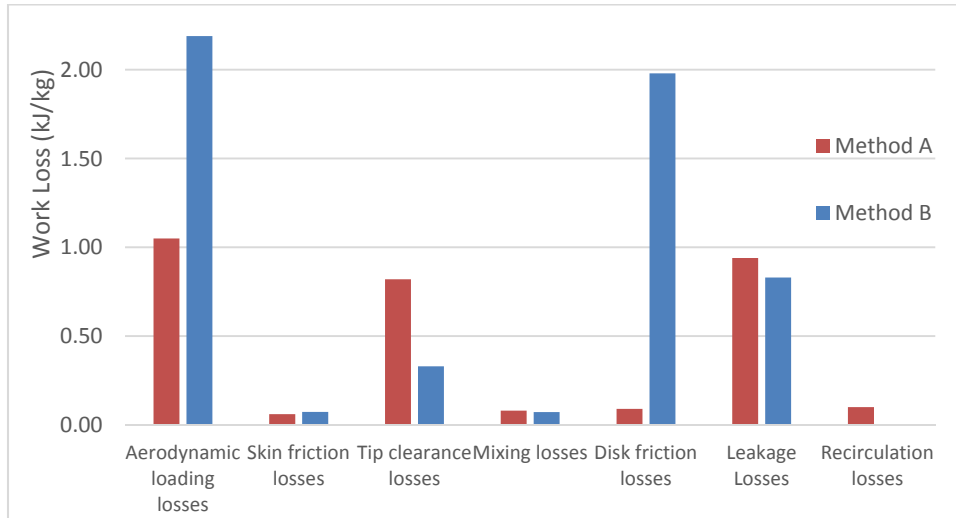
Figure 9. Comparison of Each Resulting Work Loss for Method A and Method B

CONCLUSION

This paper presents comparison of two methods for one-dimensional analysis of a centrifugal impeller; (Method A) impeller analysis based majorly on work losses, (Method B) impeller analysis accounting relative total pressure losses along with work losses. The comparison study mainly focuses on methodology to calculate internal and parasitic losses and their effects on efficiency, total pressure ratio and input power required to drive the impeller. A 100 MW closed loop S-CO$_2$ RRC Brayton Cycle is considered which yields impeller inlet conditions. Initialization of iterative process for loss calculation using isentropic impeller exit conditions is kept common for both the methods so that primary focus of comparison stays on loss calculations. The main conclusions of this study are as follows:

1. The mean line analysis codes developed give an estimate of impeller efficiency, total pressure ratio and input power required with inputs as impeller inlet conditions and RPM.
2. For the same value of RPM and geometrical parameters, the mean line analysis for method A and method B results in impeller total pressure ratio of 2.46 and 2 respectively. This reflects from the fact that method A computes work losses only and does not include pressure losses while method B accounts for pressure losses and updates the impeller exit total pressure. The higher pressure ratio for method A also results in a higher power input requirement as compared to method B.
3. For both the methods aerodynamic loading is observed to contribute the most towards losses with lower contributions of skin friction losses, mixing losses and recirculation losses. The most remarkable difference between two methods is in the calculation of recirculation losses. Method B considers a condition for recirculation to take place but method A does not. This ultimately gives a finite value for recirculation losses for method A but zero recirculation losses for method B. Contribution of disk friction losses is also significantly higher for method B than method A. Disk friction being a parasitic loss results in a large difference in design efficiency for the two methods.

17

4. Method A gives higher values for both of the described efficiencies than method B which reflects from the fact that the total amount of losses is higher for method B than method A.

The mean line analysis codes mentioned in the presented work enables users to get estimates of pressure ratio, power required and total-to-total efficiency based on RPM and inlet conditions for a single stage centrifugal compressor. This performance analysis model developed can further be used to develop an inverse code to obtain geometrical parameters for S-CO$_2$ centrifugal compressor impellers based on required pressure ratio and power input limit. For future studies, the 1-D loss models can be compared to more complex numerical methods, such as three dimensional computational fluid dynamics.

NOMENCLATURE

Ω	=	Rotation Speed, 1/s
η	=	Efficiency
ω	=	Internal Loss coefficients
λ	=	Distortion Factor
ε	=	Impeller Mean Line Radius Ratio
ε_{wake}	=	Wake friction
λ_S	=	Swirl parameter
δ_{TCL}	=	Tip Clearance Gap
ρ	=	Density, kg/m3
b	=	Blade height, m
C	=	Axial Flow Absolute Velocity, m/s
C_{MD}	=	Disk Friction Torque Coefficient
D_f	=	Diffusion Factor
D_h	=	Hydraulic Diameter, m
f_{DF}	=	Friction Factor
h	=	Specific enthalpy, kJ/kg
I	=	Work input coefficients
L	=	Length
$\dot{m}$	=	Mass Flow Rate, kg/s
P	=	Pressure, MPa
Q	=	Volumetric flow rate, m^3/s
r	=	Radius, m
s	=	Specific entropy, kJ/kg
T	=	Temperature, K
U	=	Blade Speed, m/s
V	=	Flow Relative Velocity, m/s
Z	=	Number of Blades in the Impeller
t	=	Blade Thickness, m
V_{CL}	=	Velocity of top gap clearance flow
$\dot{m}_{CL}$	=	Blade Tip Gap Leakage Mass Flow Rate
ΔZ	=	Axial Length of Impeller

Subscripts

0	=	Total or Stagnation state
1	=	Impeller inlet
2	=	Impeller exit
ABL	=	Aerodynamic Loading
b	=	Blade
corr	=	Correction
DF	=	Disk Friction
h	=	Impeller hub
id	=	Value at ideal state
lim	=	Limit
LL	=	Leakage
m	=	meridional
MIX	=	Mixing
R	=	Relative
RC	=	Recirculation
r	=	Radial component
S	=	Value at ideal state
SF	=	Skin Friction
s	=	Impeller Shroud
TCL	=	Tip Clearance Loss
w	=	Tangential component
z	=	Axial component

REFERENCES

[1] Turchi, C. S., Ma, Z., and Dyreby, J., "Supercritical Carbon Dioxide Power Cycle Configurations for use in Concentrating Solar Power Systems." *ASME Turbo Expo*, ASME, Copenhagen, Denmark, June 2012

[2] Dostal, V., Hejzlar, P., and Driscoll, M. J., "High Performance Supercritical Carbon Dioxide Cycle for Next-Generation Nuclear Reactors." *Nuclear Reactors,* Vol. 154, June 2006.

[3] Mohagheghi, M., Kapat, J., "Thermodynamic Optimization of Recuperated S-CO_2 Brayton Cycles for Solar Tower Applications," *ASME Turbo Expo,* ASME, San Antonio, TX, 2013

[4] Dostal V., Driscoll, M. J., Hejzlar, P., "A Supercritical Carbon Dioxide Cycle for Next Generation Nuclear Reactors," Advanced Nuclear Power Technology Program, MIT-ANP-TR-100, Massachusetts Institute of Technology, Cambridge, MA, 2004.

[5] Mohagheghi, M., Kapat, J., Narasimha, N., "Pareto Based Multi-Objective Optimization of Recuperated S-CO_2 Brayton Cycles." *ASME Turbo Expo*, ASME, Dusseldorf, Germany, 2014

[6] Schmitt, J., Willis, R., Amos, D., Kapat, J., Custer, C., "Study of a Supercritical CO_2 Turbine with TIT of 1350 K for Brayton Cycle with 100 MW Class Output: Aerodynamic Analysis of Stage 1 Vane" *The 4th International Symposium- Supercritical CO_2 Power Cycles,* Pittsburgh, Pennsylvania, September 2014

[7]Carlson, M. D., Kruizenga, A. K., Schalansky, C., Fleming, D. F., "Sandia Progress on Advanced Heat Exchangers for SCO2 Brayton Cycles," *The 4th International Symposium- Supercritical CO₂ Power Cycles,* Pittsburgh, Pennsylvania, September 2014

[8]Brenes, B. M., "Design of Supercritical Carbon Dioxide Centrifugal Compressors," Ph.D. Dissertation, Group of Machines and Motor of Seville, University of Seville, Seville, Spain, 2014.

[9]Wright, S. A., Radel, R. F., Vernon, M. E., Rochau, G. E., Pickard, S. P., "Operation and Analysis of a Supercritical CO2 Brayton Cycle," SAND2010-0171, Sandia National Laboratory, Albuquerque, Mexico, and Livermore, California, 2010

[10]Sanghera, S.S., "Centrifugal Compressor Mean line Design Using Real Gas Properties," DR4907-1213-PRFSS-001, Department of Mechanical and Aerospace Engineering, Carleton University, Ottawa, Ontario, Canada, 2013

[11]MATLAB and Statistics Toolbox, Ver. R2014a, The MathWorks, Inc., Natick, MA, 2014

[12]Lemmon, E. W., Huber, M. L., McLinden, M. O., NIST Standard Reference Database 23, Reference Fluid Thermodynamic and Transport Properties- REFPROP, Ver. 9.1, National Institute of Standards and Technology, Standard Reference Data Program, Gaithersburg, MD, 2013.

[13]Jansen, W., "A Method for Calculating the Flow in a Centrifugal Impeller when Entropy Gradients are present," Royal Society Conference on Internal Aerodynamics (Turbomachinery), (IME), 1967.

[14]Coppage, J.E., Dallenbach, F., Eichenberger, H.P., Hlavaka, G.E., Knoernschild, E.M. and Van Lee, N., "Study of Supersonic Radial Compressors for Refrigeration and Pressurization Systems," WADC-TR-55-257, 1956

[15]Schlichting, H., *Boundary-Layer Theory*, 7th ed., McGraw-Hill, New York, 1979, pp. 145-156.

[16]Johnston, J.P., and Dean Jr., R.C., "Losses in Vaneless Diffusers of Centrifugal Compressors and Pumps," ASME Journal of Engineering for Power, Vol 88, pp. 49-62, 1966.

[17]Lieblein, S., Schwenk, F.C., and Broderick, R.L., "Diffusion factor for estimating losses and limiting blade loadings in axial-flow-compressor blade elements," NACA RM E53D01, 1953.

[18]Daily, J.W., and Nece, R.E., "Chamber Dimension Effects on Induced Flow and Frictional Resistance of Enclosed Rotating Disks," Trans. ASME, Journal of Basic Engineering, 1960, Vol. 82, pp. 217-232.

[19]Oh, H.W., Yoon, E.S., Chung, M.K., "An optimum set of loss models for performance prediction of centrifugal compressors," Proc. Inst. Mech. Eng. Part A J. Power Energy, Vol. 211, 1997, pp. 331–338.

[20]Wiesner, F.J., "A review of slip factors for centrifugal impellers," Trans. ASME, Journal of Engineering for Power, Vol. 89, 1967, pp. 558–572.

[21]Aungier, R.H., *Centrifugal Compressors: A Strategy for Aerodynamic Design and Analysis*, ASME Press, New York, 2000

[22]Benedict, R. P., Carlucci, N. A., and Swetz, S. D., "Flow Losses in Abrupt Enlargements and Contractions," Trans. ASME, Journal of Engineering for Power, January, 1996, pp. 73-81.

[23]Aungier, R. H., "Mean Streamline Aerodynamic Performance Analysis of Centrifugal Compressors," Trans. ASME, Journal of Turbomachinery, 1995, Vol. 117, pp. 360-366.